

Endogenous Precision of the Number Sense

Arthur Prat-Carrabin^{1,†,*} and Michael Woodford¹

¹Department of Economics, Columbia University, New York, USA

[†]*Present address:* Department of Psychology, Harvard University, Cambridge, USA

^{*}*email:* arthurpc@fas.harvard.edu

April 10, 2024

Abstract

The behavioral variability in psychophysical experiments and the stochasticity of sensory neurons have revealed the inherent imprecision in the brain’s representations of environmental variables. Numerosity studies yield similar results, pointing to an imprecise ‘number sense’ in the brain. If the imprecision in representations reflects an optimal allocation of limited cognitive resources, as suggested by efficient-coding models, then it should depend on the context in which representations are elicited. Through an estimation task and a discrimination task, both involving numerosities, we show that the scale of subjects’ imprecision increases, but sublinearly, with the width of the prior distribution from which numbers are sampled. This sublinear relation is notably different in the two tasks. The double dependence of the imprecision — both on the prior and on the task — is consistent with the optimization of a tradeoff between the expected reward, different for each task, and a resource cost of the encoding neurons’ activity. Comparing the two tasks allows us to clarify the form of the resource constraint. Our results suggest that perceptual noise is endogenously determined, and that the precision of percepts varies both with the context in which they are elicited, and with the observer’s objective.

Significance statement

Results in neuroscience and psychology have suggested that the precision with which we represent the important variables of our environment, including numbers, proceeds from an optimized tradeoff between the objective and the cost of our representations. But the nature of this objective and of this cost remain unclear. By comparing the behavioral variability obtained in two experiments, and using several different ranges of numbers, we show that human observers optimize the objective of their current task (instead of a general-purpose objective, as often assumed), under a resource cost of the encoding neurons. This results in sublinear scaling laws, obtained in data, relating the degree of imprecision of internal representations to the range of stimuli expected in a given context.

34 Quartz wristwatches gain or lose about half a second every day. Still, they are useful for
35 what one typically needs to know about the time, and they sell for as low as five dollars.
36 The most recent atomic clocks carry an error of less than one second over the age of the
37 Universe, and they are used to detect the effect of Einstein’s theory of general relativity at a
38 millimeter scale¹; but they are much more expensive. Precision comes at a cost, and the kind
39 of cost that one is willing to bear depends on one’s objective. Here we argue that in order to
40 make the many decisions that stipple our daily lives, the brain faces—and rationally solves—
41 similar tradeoff problems, which we describe formally, between an objective that may vary
42 with the context, and a cost on the precision of its internal representations about external
43 information.

44 As a considerable fraction of our decisions hinges on our appreciation of environmental
45 variables, it is a matter of central interest to understand the brain’s internal representations
46 of these variables—and the factors that determine their precision. An almost invariable
47 behavioral pattern, in more than a century of studies in psychophysics, is that the responses
48 of subjects exhibit variability across repeated trials. This variability has increasingly been
49 thought to reflect the randomness in the brain’s representations of the magnitudes of the
50 experimental stimuli^{2–4}. Substantiating this view, studies in neuroscience exhibit how many
51 of these representations seem to materialize in the activity of populations of neurons, whose
52 patterns of firing of action potentials (electric signals) are well described by Poisson processes:
53 typically, average firing rates are functions (‘tuning curves’) of the stimulus magnitude, which
54 is therefore ‘encoded’ in an ensemble of action potentials, i.e., in a stochastic, and thus
55 imprecise, fashion^{5–7}. Similar results have been obtained in studies on the perception of
56 numerical magnitudes. People are imprecise, when asked to estimate the ‘ numerosity ’ of an
57 array of items, or in tasks involving Arabic numerals^{8,9}; and the tuning curves of number-
58 selective neurons in the brains of humans and monkeys have been exhibited^{10,11}. These
59 findings point to the existence of a ‘ number sense ’ that endows humans (and some animals)

60 with the ability to represent, imprecisely, numerical magnitudes¹².

61 The quality of neural representations depends on the number of neurons dedicated to
62 the encoding, on the specifics of their tuning curves, and on the duration for which they
63 are probed. Models of *efficient coding* propose, as a guiding principle, that the encoding
64 optimizes some measure of the fidelity of the representation, under a constraint on the
65 available encoding resources^{13–25}. While they make several successful predictions (e.g., more
66 frequent stimuli are encoded with higher precision^{16,19,20,25,26}), including in the numerosity
67 domain^{27,28}, several aspects of these models remain subject to debate^{29,30}, although they
68 shape crucial features of the predicted representations. First, in many studies, the encoding
69 is assumed to optimize the mutual information between the external stimulus and the internal
70 representations^{18–20,22}, but it is seldom the case that this is actually the objective that an
71 observer needs to optimize. An alternative possibility is that the encoding optimizes the
72 observer’s current objective, which may vary depending on the task at hand^{24,31}. Second,
73 the nature of the resource that constrains the encoding is also unclear, and several possible
74 limiting quantities are suggested in the literature (e.g., the expected spike rate, the number
75 of neurons^{16,17,20}, or a functional on the Fisher information, a statistical measure of the
76 encoding precision^{18,19,21,23,24}). Third, most studies posit that the resource in question is
77 costless, up to a certain bound beyond which the resource becomes depleted. Another
78 possibility is that there is a cost that increases with increasing utilization of the resource
79 (e.g., action potentials come with a metabolic cost^{32–34}). Together, these aspects determine
80 how the optimal encoding, and thus the resulting behavior, depend on the task and on the
81 ‘prior’ (the stimulus distribution).

82 Hence we shed light on all three questions by manipulating, in experiments, the task and
83 the prior. In an estimation task, subjects estimate the numbers of dots in briefly presented
84 arrays. In a discrimination task, subjects see two series of numbers and are asked to choose
85 the one with the highest average. In both tasks, experimental conditions differ by the size of
86 the range of numbers that are presented to subjects (i.e., by the width of the prior). In each

87 case we examine closely the variability of the subjects’ responses. We find that it depends on
88 both the task and the prior. The scale of the subjects’ imprecision increases *sublinearly* with
89 the width of the prior, and this sublinear relation is different in the two tasks. We reject
90 ‘normalization’ accounts of the behavioral variability, and in the estimation task we find no
91 evidence of ‘scalar variability’, whereby the standard deviation of estimates for a number is
92 proportional to the number, as sometimes reported in numerosity studies. The behavioral
93 patterns we exhibit are predicted by a model in which the imprecision in representations is
94 adapted to the observer’s current task, whose expected reward it optimizes under a resource
95 cost on the activity of the encoding neurons. The subjects’ imprecision is thus endogenously
96 determined, through the rational allocation of costly encoding resources.

97 Our experimental results suggest, at least in the numerosity domain, a behavioral regu-
98 larity — a task-dependent quantitative law of the scaling of the responses’ variability with
99 the range of the prior — for which we provide a resource-rational account. Below, we present
100 the results pertaining to the estimation task, followed by those of the discrimination task,
101 before turning to our theoretical account of these experimental findings. The results we
102 present here are obtained by pooling together the responses of the subjects; the analysis of
103 individual data further substantiates our conclusions (see [Methods](#)).

104 **Estimation task**

105 In each trial of a numerosity estimation task, subjects are asked to provide their best estimate
106 of the number of dots contained in an array of dots presented for 500ms on a computer screen
107 (Fig. 1a). In all trials, the number of dots is randomly sampled from a uniform distribution,
108 hereafter called ‘the prior’, but the width of the prior, w , is different in three experimental
109 conditions. In the ‘Narrow’ condition, the range of the prior is $[50, 70]$ (thus the width w
110 is 20); in the ‘Medium’ condition, the range is $[40, 80]$ (thus $w = 40$); and in the ‘Wide’
111 condition, the range is $[30, 90]$ (thus $w = 60$; Fig. 1b). In all three conditions the mean
112 of the prior (which is the middle of the range) is 60. As an incentive, the subjects receive

113 for each trial a financial reward which decreases linearly with the square of their estimation
114 error. Each condition comprises 120 trials, and thus often the same number is presented
115 multiple times, but in these cases the subjects do not always provide the same estimates.
116 We now examine this variability in subjects' responses.

117 Studies on numerosity estimation with similar stimuli sometimes report that the standard
118 deviation of estimates increases proportionally to the estimated number. This property,
119 dubbed 'scalar variability', has been seen as a signature of numerical-estimation tasks, and
120 more generally, of the 'number sense'³⁵. However, looking at the standard deviation of
121 estimates as a function of the presented number, we find that it is not well described by an
122 increasing line. In the three conditions, the standard deviation seems to be maximal near
123 the center of the range (60), and to slightly decrease for numbers closer to the boundaries
124 of the prior (Fig. 1c). Dividing each prior range in five bins of similar sizes, we compute
125 the variance of estimates in each bin (see [Methods](#)). In the three conditions, the variance
126 in the middle (third) bin is greater than the variances in the fourth and fifth bins (which
127 contain larger numbers). These differences are significant (p-values of Levene's tests of
128 equality of variances: third vs. fifth bin, largest p-v. across the three conditions: 5e-6; third
129 vs. fourth bin, Narrow condition: 0.009, Medium condition: 1.2e-5) except between the third
130 and fourth bin in the Wide condition (p-v.: 0.12). This substantiates the conclusion that the
131 standard deviation of estimates is not an increasing linear function of the number. Moreover,
132 a hallmark of scalar variability is that the 'coefficient of variation', defined as the ratio of
133 the standard deviation of estimates to the mean estimate, is constant³⁵. We find that in our
134 experiment, it is decreasing for most of the numbers, in the three conditions (Fig. 1e); this
135 is consistent with the results of Ref.³⁶. We conclude that the scalar-variability property is
136 not verified in our data.

137 In fact, the most striking feature of the variability of estimates is not how it depends
138 on the number, but how it strongly depends on the width of the prior, w (Fig. 1c,d). For
139 instance, with the numerosity 60, the standard deviation of subjects' estimates is 4.2 in the

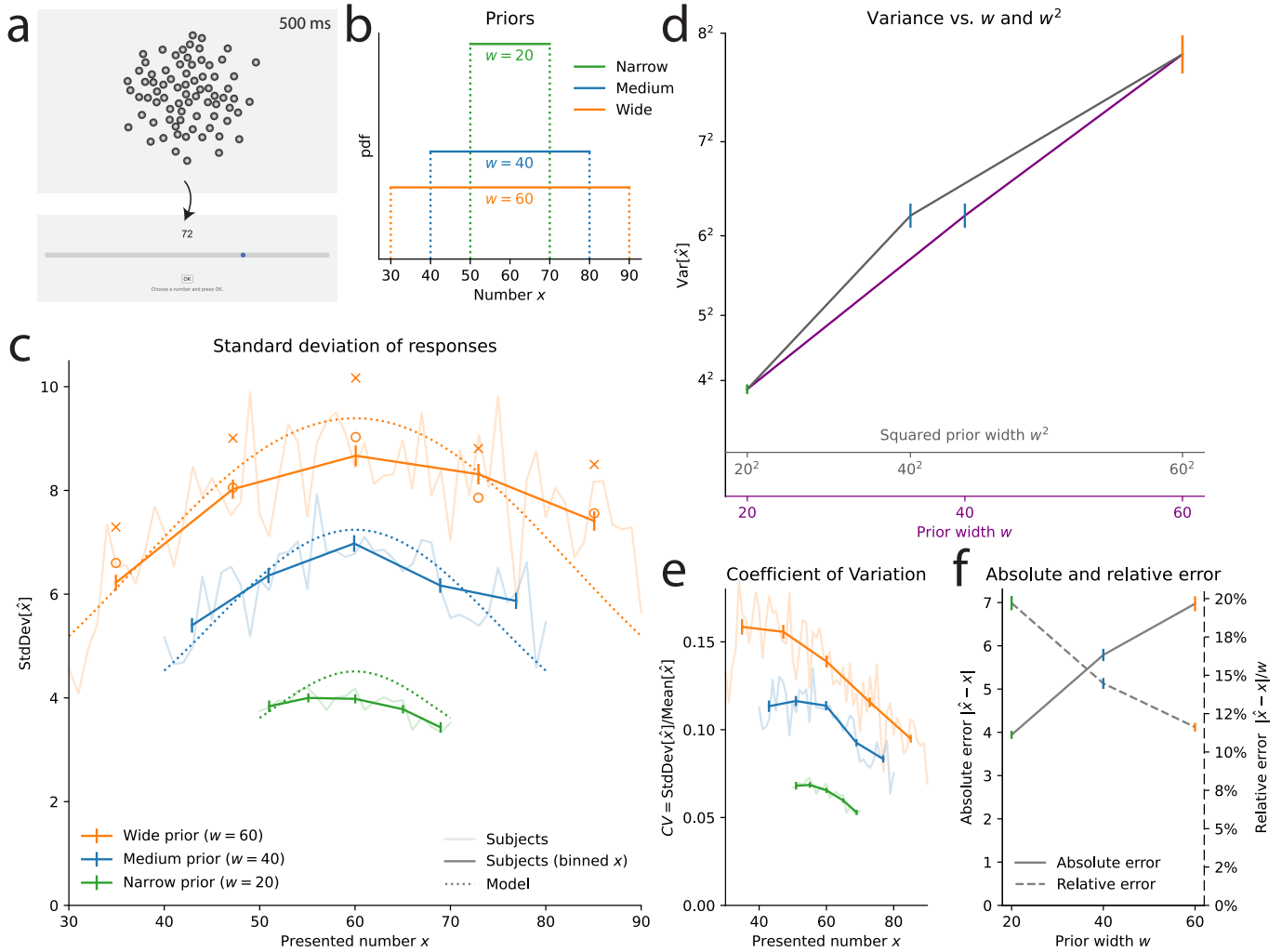


Fig. 1. Estimation task: the scale of subjects’ imprecision increases sublinearly with the prior width.

a. Illustration of the estimation task: in each trial, a cloud of dots is presented on screen for 500ms. Subjects are then asked to provide their best estimate of the number of dots shown. **b.** Uniform prior distributions (from which the numbers of dots are sampled) in the three conditions of the task. **c.** Standard deviation of the responses of the subjects (solid lines) and of the best-fitting model (dotted lines), as a function of the number of presented dots, in the three conditions. For each prior, five bins of approximately equal sizes are defined; subjects’ responses to the numbers falling in each bin are pooled together (thick lines) or not (thin lines). **d.** Variance of subjects’ responses, as a function of the width of the prior (purple line) and of the squared width (grey line). Both lines show the same data; only the x-axis scale has been changed. **e.** Subjects’ coefficients of variations, defined as the ratio of the standard deviation of estimates over the mean estimate, as a function of the presented number, in the three conditions. **f.** Absolute error (solid line), defined as the absolute difference between a subject’s estimate and the correct number, and relative error (dashed line), defined as the ratio of the absolute error to the prior width, as a function of the prior width. In panels **c-d**, the responses of all the subjects are pooled together; error bars show twice the standard errors.

140 Narrow condition, 6.8 in the Medium condition, and 8.4 in the Wide condition, although
 141 these estimates were all obtained after the presentations of the same number of dots (60).
 142 Testing for the equality of the variances of estimates across the three conditions, for each
 143 number contained in all three priors (i.e., all the numbers in the Narrow range,) we find
 144 that the three variances are significantly different, for all the numbers (largest Levene’s test
 145 p-value, across the numbers: 1e-7, median: 2e-15).

146 The variability of estimates increases with the width of the prior. This suggests that
 147 the imprecision in the internal representation of a number is larger when a larger range of
 148 numbers needs to be represented. This would be the case if internal representations relied
 149 on a mapping of the range of numbers to a normalized, bounded internal scale, and the
 150 estimate of a number resulted from a noisy readout (or a noisy storage) on this scale, as in
 151 ‘range-normalization’ models^{37–42}. Consider for instance the representation of a number x ,
 152 obtained through its normalization onto the unit range $[0, 1]$, and then read with noise, as

$$r = \frac{x - x_{min}}{w} + \varepsilon, \tag{1}$$

153 where x_{min} is the lowest value of the prior, and ε a centered normal random variable with
 154 variance ν^2 . Suppose that the estimate, \hat{x} , is obtained by rescaling the noisy representation
 155 back to the original range, i.e., $\hat{x} = x_{min} + rw$ (we make this assumption for the sake of
 156 simplicity, but the argument we develop here is equally relevant for the more elaborate,
 157 Bayesian model we present below). The scale of the noise, given by ν , is constant in the
 158 normalized scale; thus in the space of estimates the noise scales with the prior width, w . If
 159 we allow, in addition to the noise in estimates, for some amount of independent motor noise
 160 of variance σ_0^2 in the responses actually chosen by the subject, we obtain a model in which
 161 the variance of responses is $\sigma_0^2 + \nu^2 w^2$, i.e., an affine function of the *square* of the width of
 162 the prior.

163 With the numerosity 60, the variance of subjects’ estimates is $4.2^2 = 17.64$ in the Narrow

164 condition ($w = 20$), and $6.8^2 = 46.24$ in the Medium condition ($w = 40$): given these two
 165 values, the affine relation just mentioned predicts that in the Wide condition ($w = 60$) the
 166 variance should be $9.7^2 = 93.91$. We find instead that it is $8.4^2 = 70.56$, i.e., about 25%
 167 lower than predicted, suggesting a sublinear relation between the variance and the square
 168 of the prior width. Indeed the variance of estimates does not seem to be an affine function
 169 of the square of the prior width (Fig. 1d, grey line and grey abscissa). Our investigations
 170 reveal that instead, the variance is significantly better captured by an affine function of the
 171 width — and not of the squared width (Fig. 1d, purple line and purple abscissa).

172 As an additional illustration of this result, for each of the five bins mentioned above and
 173 defined for the three priors, we compute the predicted variance of estimates in the Wide
 174 condition on the basis of the variances in the Narrow and Medium conditions, and resulting
 175 either from the hypothesis of an affine function of the squared width, $\sigma_0^2 + \nu^2 w^2$, or from
 176 the hypothesis of an affine function of the width, $\sigma_0^2 + \nu^2 w$. The variances predicted with
 177 the former hypothesis all overestimate the variances of subjects' responses (Fig. 1c, orange
 178 crosses), but the predictions of the latter hypothesis appear consistent with the behavioral
 179 data (Fig. 1c, orange circles).

180 We further investigate how the imprecision in internal representations depends on the
 181 width of the prior through a behavioral model in which responses results from a stochastic
 182 encoding of the numerosity, followed by a Bayesian decoding step. Specifically, the pre-
 183 sentation of a number x results in an internal representation, r , drawn from a Gaussian
 184 distribution with mean x and whose standard deviation, νw^α , is proportional to the prior
 185 width raised to the power α ; i.e., $r|x \sim N(x, \nu^2 w^{2\alpha})$, where ν is a positive parameter that
 186 determines the baseline degree of imprecision in the representation, and α is a non-negative
 187 exponent that governs the dependence of the imprecision on the width of the prior. The
 188 observer derives, from the internal representation r , the mean of the Bayesian posterior over
 189 x , $x^*(r) \equiv \mathbb{E}[x|r]$. We note that this estimate minimizes the squared-error loss, and thus
 190 maximizes the expected reward in the task. The selection of a response includes an amount

191 of motor noise: the response, \hat{x} , is drawn from a Gaussian distribution centered on the
192 Bayesian estimate, $x^*(r)$, with variance σ_0^2 , truncated to the prior range, and rounded to the
193 nearest integer. This model has three parameters (σ_0 , ν , and α).

194 The likelihood of the model is maximized for $\alpha = 0.48$, a value close to $1/2$ (and less close
195 to 1), suggesting that the standard deviation is approximately a linear function of \sqrt{w} (and
196 the variance a linear function of w). The nested model obtained by fixing $\alpha = 1/2$ yields a
197 slightly poorer fit (which is expected for a nested model), but the difference in log-likelihood
198 is small (0.38), and the Bayesian Information Criterion (BIC), a measure of fit that penalizes
199 larger numbers of parameters⁴³, is lower (i.e., better) by 8.70 for the constrained model with
200 $\alpha = 1/2$. This indicates that setting $\alpha = 1/2$ provides a parsimonious fit to the data that is
201 not significantly improved by allowing α to differ from $1/2$. A different specification, $\alpha = 1$,
202 corresponds to a normalization model similar to the one described above, but here with a
203 Bayesian decoding of the internal representation. The BIC of this model is higher by 244
204 than that with $\alpha = 1/2$, indicating a much worse fit to the data. (Throughout, we report
205 the models' BICs even if they have the same number of parameters, so as to compare the
206 values of a single metric). We emphasize that this large difference in BIC implies that the
207 hypothesis $\alpha = 1$ can be confidently rejected, in favor of the hypothesis $\alpha = 1/2$ (in informal
208 terms, it is not the case that the grey line in Fig. 1d, showing the variance vs. the squared
209 width, only appears curved because of some sampling noise, in fact it is indeed *not* a straight
210 line; while it is substantially more probable that the purple one, showing the variance vs.
211 the width, corresponds indeed to a straight line).

212 The standard deviation of representations thus seems to increase linearly with the square
213 root of the prior width, \sqrt{w} . The positive dependence results in larger errors when the prior
214 is wider (Fig. 1f, solid line). But the sublinear relation implies that the subjects in fact make
215 smaller *relative* errors (relatively to the width of the prior), when the prior is wider. In the
216 Narrow condition, the ratio of the average absolute error to the width of the prior, $\frac{|\hat{x}-x|}{w}$,
217 is 19.7%, i.e., the size of errors is about one fifth of the prior width. This ratio decreases

218 substantially, to 14.5% and 11.6% in the Medium and Wide conditions, respectively, i.e., the
219 size of errors is about one ninth of the prior width in the Wide condition (Fig. 1f, dashed
220 line). In other words, while the size of the prior is multiplied by 3, the relative size of errors
221 is multiplied by $\frac{5}{9} \simeq 0.56$, and thus the absolute size of errors is multiplied by $3 \cdot \frac{5}{9} \simeq 1.67$. If
222 subjects had the same relative sizes of errors in both the Narrow and the Wide conditions,
223 their absolute error would be multiplied by 3; conversely the absolute error would be the
224 same in the two conditions if the relative error was divided by 3. The behavior of subjects
225 falls in between these two scenarios: they adopt smaller relative errors in the Wide condition,
226 although not so much so as to reach the same absolute error as in the Narrow condition.
227 Below, we show how this behavior is accounted for by a tradeoff between the performance
228 in the task and a resource cost on the activity of the mobilized neurons. But first, we ask
229 whether subjects exhibit, in a discrimination task, the same sublinear relation between the
230 imprecision of representations and the width of the prior.

231 **Discrimination task**

232 In many decision situations, instead of providing an estimate, one is required to select the
233 better of two options. We thus investigate experimentally the behavior of subjects in a
234 discrimination task. In each trial, subjects are presented with two interleaved series of
235 numbers, five red and five blue numbers, after which they are asked to choose the series
236 that had the higher average (Fig. 2a). Each number is shown for 500ms. Two experimental
237 conditions differ by the width of the uniform prior from which the numbers (both blue and
238 red) are sampled: in the Narrow condition the range of the prior is $[35, 65]$ (the width of
239 the prior is thus $w = 30$) and in the Wide condition the range is $[10, 90]$ (the width is thus
240 $w = 80$; Fig. 2b). After each decision, subjects receive a number of points equal to the
241 average that they chose. At the end of the experiment, the total sum of their points is
242 converted to a financial reward (through an increasing affine function).

243 Subjects in this experiment sometimes make incorrect choices (i.e., they choose the color

244 whose numbers had the lower average), but they make less incorrect choices when the dif-
 245 ference between the two averages is larger, and the proportion of trials in which they choose
 246 ‘red’ is a sigmoid function of the difference between the average of the red numbers, x_R ,
 247 and the average of the blue numbers, x_B (Fig. 2c). In the Narrow condition, this proportion
 248 reaches 60% when the difference in the averages is 1, and 90% when the difference is 7. In
 249 the Wide condition, we find that the slope of this psychometric curve is less steep: subjects
 250 reach the same two proportions for differences of about 2.4 and 12.6, respectively.

251 In the Wide condition, it thus requires a larger difference between the red and blue aver-
 252 ages for the subjects to reach the same discrimination threshold; put another way, the same
 253 difference in the averages results in more incorrect choices in the Wide condition than in the
 254 Narrow condition. As with the estimation task, this suggests that the degree of imprecision
 255 in representations is larger when the range of numbers that must be represented is larger.
 256 To estimate this quantitatively, we turn to the predictions of the model presented above,
 257 here considered in the context of the discrimination task: in this model, the average x_C ,
 258 where C is ‘blue’ or ‘red’ (denoted by B and R , respectively), results in an internal repre-
 259 sentation, r_C , drawn from a Gaussian distribution with mean x_C and whose variance, $\nu^2 w^{2\alpha}$,
 260 is proportional to the prior width raised to the exponent 2α , i.e., $r_C|x_C \sim N(x_C, \nu^2 w^{2\alpha})$.
 261 Given the (independent) representations r_B and r_R , the subject, optimally, compares the
 262 Bayesian estimates for each quantity, $x^*(r_B)$ and $x^*(r_R)$, and chooses the greater one. As
 263 the Bayesian estimate is an increasing function of the representation, the probability that
 264 the subject choose ‘red’, conditional on two averages x_B and x_R , is the probability that r_R
 265 be larger than r_B , i.e.,

$$P(\text{‘red’}|x_B, x_R) = P(r_R > r_B|x_B, x_R) = \Phi\left(\frac{x_R - x_B}{\sqrt{2\nu w^\alpha}}\right), \quad (2)$$

266 where Φ is the cumulative distribution function of the standard normal distribution.

267 The choice probability is thus predicted to be a function of the ratio $\frac{x_R - x_B}{w^\alpha}$ of the dif-

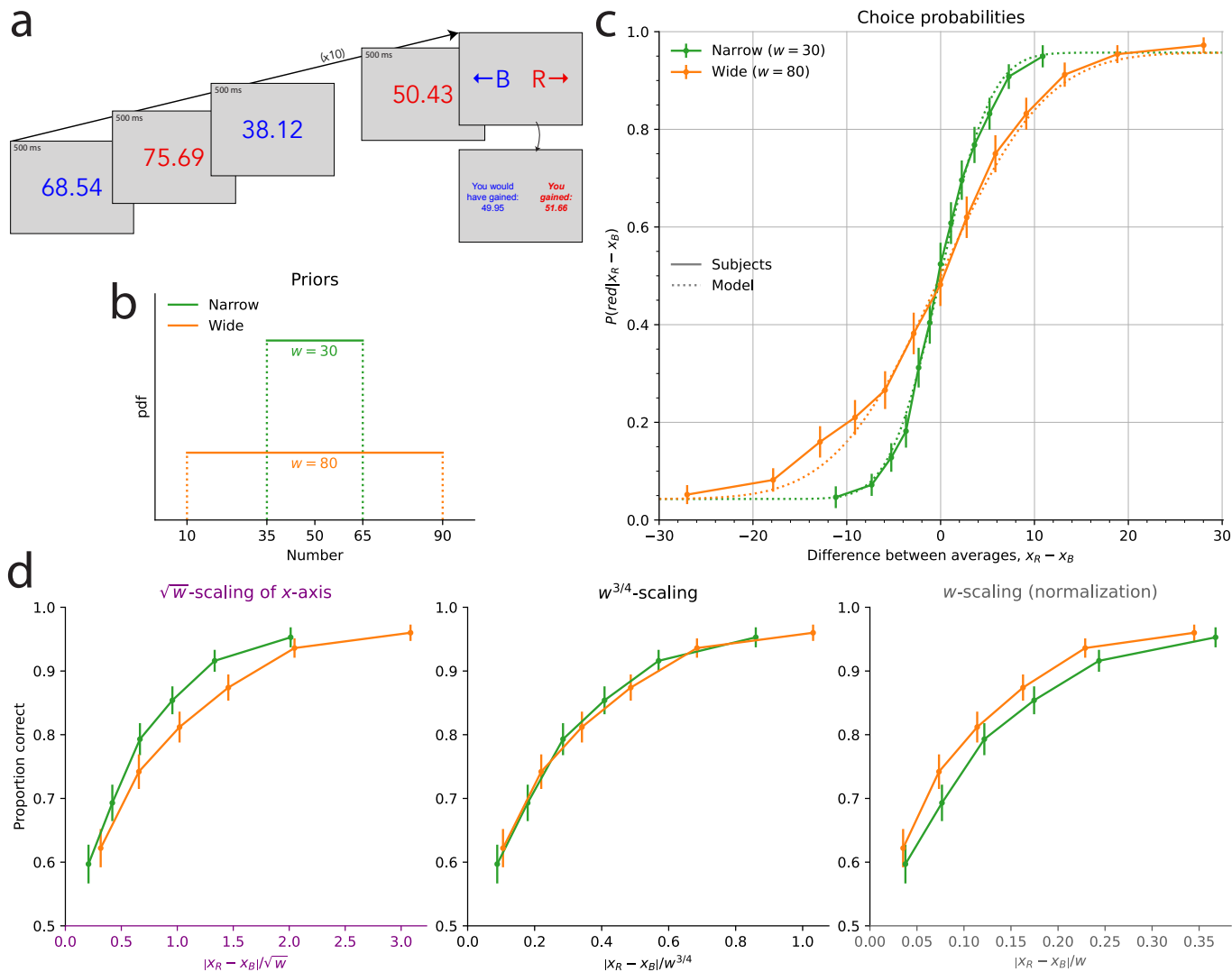


Fig. 2. Discrimination task: the scale of subjects’ imprecision increases with the prior width; the relation is sublinear, but different than in the estimation task. **a.** Illustration of the discrimination task: in each trial, subjects are shown five blue numbers and five red numbers, alternating in color, each for 500ms, after which they are asked to choose the color whose numbers have the higher average. **b.** Uniform prior distributions (from which the numbers of dots are sampled) in the two conditions of the task. **c.** Proportion of choices ‘red’ in the responses of the subjects (solid lines) and of the best-fitting model (dotted lines), as a function of the difference between the two averages, in the two conditions. **d.** Proportion of correct choices in subjects’ responses as a function of the absolute difference between the two averages divided by the square root of the prior width (left), by the prior width raised to the power 3/4 (middle), and by the prior width (right). The three subpanels are different representations of the same data. In panels **c** and **d**, the responses of all the subjects are pooled together; error bars show the 95% confidence intervals.

268 ference between the two averages over the width of the prior raised to the power α , and
269 therefore the same choice probability should be obtained across conditions as long as this
270 ratio is the same. In Figure 2d, we show for different values of α the subjects' proportions
271 of correct responses as a function of the absolute value of this ratio, so as to be able to ex-
272 amine closely the difference between the resulting choice curves in the two conditions. The
273 case $\alpha = 1$ corresponds, as above, to the hypothesis that the standard deviation of internal
274 representations is a linear function of the width, w , i.e., a normalization of the numbers by
275 the width of the prior. But we find that the proportion of correct choices as a function of the
276 ratio $|x_R - x_B|/w$ is greater in the Wide condition than in the Narrow condition (Fig. 2d,
277 last panel). In other words, in the Wide condition the subjects are more sensitive to the
278 normalized difference than in the Narrow condition. This suggests that between the Narrow
279 and the Wide conditions, the imprecision in representations does not change in the same
280 proportions as does the prior width; specifically, it suggests a sublinear relation between the
281 scale of the imprecision and the width of the prior.

282 As seen in the previous section, the behavioral data in the estimation task precisely
283 suggest such a sublinear relation, and more precisely point to the exponent $\alpha = 1/2$, i.e., to
284 a linear relation between the standard deviation and the square-root of the width, \sqrt{w} . But
285 the proportion of correct choices as a function of the corresponding ratio, $|x_R - x_B|/\sqrt{w}$,
286 is greater in the Narrow condition than in the Wide condition (Fig. 2d, first panel). The
287 sublinear relation, thus, is not the same in the two tasks; and the data suggest in the case of
288 the discrimination task an exponent α greater than $1/2$, but lower than 1. Indeed, we find
289 that the choice curves in the two conditions match very well with $\alpha = 3/4$ (Fig. 2d, middle
290 panel).

291 Model fitting substantiates this result. We add to our model (in which the probability of
292 choosing 'red' is given by Eq. 2) the possibility of 'lapse' events, in which either response is
293 chosen with probability 50%; an additional parameter, η , governs the probability of lapses.
294 (We reach the same conclusions with a model with no lapse, but this model with lapses yields

295 a better fit; see [Methods](#).) The BIC of this model with $\alpha = 3/4$ is lower (i.e., better) by
296 44.1 than that with $\alpha = 1/2$, and by 18.3 than that with $\alpha = 1$, indicating strong evidence
297 rejecting the hypotheses $\alpha = 1/2$ and $\alpha = 1$, in favor instead of the hypothesis of an exponent
298 α equal to $3/4$. Notwithstanding the theoretical reasons, presented below, that motivate our
299 focus on this specific value of the exponent in addition to the good fit to the data, we can
300 let α be a free parameter, in which case its best-fitting value is 0.80 (and thus close to $3/4$).
301 This model’s BIC is however higher (i.e., worse) by 7.9 than that of the model with α fixed
302 at $3/4$, which indicates strong evidence⁴⁴ in favor of the equality $\alpha = 3/4$. In sum, our
303 best-fitting model is one in which the standard deviation of the internal representations is a
304 linear function of the prior width raised to the power $3/4$. As with the estimation task, this
305 sublinear relation implies that subjects are relatively more precise when the prior is wider.
306 This allows them to achieve a significantly better performance in the Wide condition than
307 in the Narrow condition (with 80.2% and 77.4% of correct responses, respectively; p-value
308 of Fisher’s exact test of equality of the proportions: 9.5e-5).

309 **Task-optimal endogenous precision**

310 The subjects’ behavioral patterns in the estimation task and in the discrimination task
311 suggest that the scale of the imprecision in their internal representations increases sublinearly
312 with the range of numerosities used in a given experimental condition. Specifically, the scale
313 of the imprecision seems to be a linear function of the prior width raised to the power $1/2$,
314 in the estimation task, and raised to the power $3/4$, in the discrimination task. We now
315 show that these two exponents, $1/2$ and $3/4$, arise naturally if one assumes that the observer
316 optimizes the expected reward in each task, while incurring a cost on the activity of the
317 neurons that encode the numerosities.

318 Inspired by models of perception in neuroscience^{16–18,20–25,45–47}, we consider a two-stage,
319 encoding-decoding model of an observer’s numerosity representation. In the encoding stage,
320 a numerosity x elicits in the brain of the observer an imprecise, stochastic representation,

321 r , while the decoding stage yields the mean of the Bayesian posterior, which is the optimal
322 decoder in both tasks. The model of Gaussian representations that we use throughout the
323 text is one example of such an encoding-decoding model.

324 The encoding mechanism is characterized by its Fisher information, $I(x)$, which reflects
325 the sensitivity of the representation’s probability distribution to changes in the stimulus x .
326 The inverse of the square-root of the Fisher information, $1/\sqrt{I(x)}$, can be understood as
327 the scale of the imprecision of the representation about a numerosity x . More precisely,
328 it is approximately — when $I(x)$ is large — the standard deviation of the Bayesian-mean
329 estimate of x derived from the encoded representation. (For smaller $I(x)$, the standard
330 deviation of the Bayesian-mean estimate increasingly depends on the shape of the prior; with
331 a uniform prior, it decreases near the boundaries.) The variability in subjects’ responses in
332 the estimation task, and their choice probabilities in the discrimination task, reported above,
333 are thus indirect measures of the Fisher information of their encoding process.

334 Moreover, the expected squared error of the Bayesian-mean estimate of x is approximately
335 the inverse of the Fisher information, $1/I(x)$. We thus consider the generalized loss function

$$L_a[I] = \int \frac{\pi(x)^a}{I(x)} dx, \quad (3)$$

336 where $\pi(x)$ is the prior distribution from which x is sampled. With $a = 1$, this quantity ap-
337 proximates the expected quadratic loss that subjects in the estimation task should minimize
338 in order to maximize their reward. And with $a = 2$, minimizing this loss is approximately
339 equivalent to maximizing the reward in the discrimination task²⁴. (The squared prior, in
340 the expression of $L_2[I]$, corresponds to the probability of the co-occurrence of two presented
341 numerosities that are close to each other, which is the kind of event most likely to result in
342 errors in discrimination.)

343 In both cases, a more precise encoding, i.e., a greater Fisher information, results in a
344 smaller loss. This precision, however, comes with a cost. We assume that the encoding

345 results from an accumulation of signals, each entailing an identical cost (e.g., the energy
 346 resources consumed by action potentials³²⁻³⁴.) The more signals the observer collects, the
 347 greater the precision; but also the greater the cost, which is proportional to the number of
 348 signals. Formally, we consider a continuum-limit model, in which a representation proceeds
 349 from a Wiener process (Brownian motion) with infinitesimal variance s^2 , observed for a
 350 duration T (the continuum equivalent of the number of collected signals). The drift of
 351 the process, $m(x)$, encodes the number: it can be, for instance, some normalized value
 352 of x ; but here we only assume that the function $m(x)$ is increasing and bounded. The
 353 resulting representation, r , is normally distributed, as $r|x \sim N(m(x)T, s^2T)$, and its Fisher
 354 information is $T(m'(x))^2/s^2$ and thus it is proportional to T . The bound on $m(x)$ puts a
 355 constraint on the Fisher information: specifically, it implies that the quantity

$$C[I] = \left(\int \sqrt{I(x)} dx \right)^2 \quad (4)$$

356 is bounded by a quantity proportional to the duration, i.e., $C[I] \leq KT$, where $K > 0$. Other
 357 studies^{18,21,24} have posited a bound on the quantity $C[I]$, but here we emphasize that the
 358 bound is a linear function of the duration of observation, and we assume, crucially, that the
 359 observer can choose this duration, T , but at the expense of a cost that is proportional to T .

360 Specifically, we assume that the observer chooses the function $I(\cdot)$ and the duration T
 361 that solve the minimization problem

$$\min_{I(\cdot), T} L_a[I] + \lambda T \quad \text{subject to } C[I] \leq KT, \quad (5)$$

362 where $\lambda > 0$. In this problem, any increase of the Fisher information, within the bound,
 363 improves the objective function; and thus the solution saturates the bound, i.e., $C[I] = KT$.
 364 Hence the problem reduces to that of choosing the function $I(\cdot)$ that solves the minimization
 365 problem

$$\min_{I(\cdot)} L_a[I] + \theta C[I], \quad (6)$$

366 where $\theta = \lambda/K$. The solution is

$$I(x) = \frac{\pi(x)^{2a/3}}{\sqrt{\theta \int \pi(\tilde{x})^{a/3} d\tilde{x}}}. \quad (7)$$

367 This implies that the optimal Fisher information vanishes outside of the support of the prior;
 368 and in the case of a uniform prior of width w , $I(x)$ is constant, as

$$\begin{aligned} I(x) &= \frac{1}{\sqrt{\theta}w} && \text{for the estimation task,} \\ \text{and } I(x) &= \frac{1}{\sqrt{\theta}w^{3/2}} && \text{for the discrimination task,} \end{aligned} \quad (8)$$

369 for any x such that $\pi(x) \neq 0$.

370 The scale of the imprecision of internal representations, $1/\sqrt{I(x)}$, is thus predicted to be
 371 proportional to the prior width raised to the power $1/2$, in the estimation task, and raised
 372 to the power $3/4$, in the discrimination task. As shown above, we find indeed that in these
 373 tasks, the imprecision of representations not only increases with the prior width, but it does
 374 so in a way that is quantitatively consistent with these two exponents. As for the model of
 375 Gaussian representations that we have considered throughout the text, it is in fact equivalent
 376 to the model just presented, up to a linear transformation of the representation that does
 377 not impact its Fisher information (nor the resulting estimates). Its Fisher information is the
 378 inverse of the variance, i.e., $1/(\nu^2 w^{2\alpha})$, and thus Eq. 8 implies $\alpha = 1/2$ for the estimation
 379 task, and $\alpha = 3/4$ for the discrimination task, i.e., the two values that indeed best fit the
 380 data.

381 Many efficient-coding models in the literature feature a different objective, the maxi-
 382 mization of the mutual information^{18–20}; but a single objective cannot explain our different
 383 findings in the two tasks (namely, the different dependence on the prior width). Many mod-
 384 els also feature a different kind of constraint: a *fixed* bound on the quantity in Eq. 4, or on
 385 a generalization of this quantity^{18,19,21,23}. But here also, as this bound is usually saturated,

386 the optimal Fisher information, which is constant, here, due to the uniform prior, is entirely
387 determined by the constraint—irrespective of the objective of the task. This hypothesis thus
388 cannot account either for the difference that we find between the two tasks. By contrast,
389 we assume that it is the task’s expected reward that is maximized, and that the amount
390 of utilized encoding resources can be endogenously determined: our model is thus able to
391 predict not only that the behavior should depend on the prior, but also that this dependence
392 should change with the task; and it makes quantitative predictions that coincide with our
393 experimental findings.

394 We compare the responses of the subjects and of the Gaussian-representation model, with
395 $\alpha = 1/2$ in the estimation task and $\alpha = 3/4$ in the discrimination task. In both cases, the
396 parameter ν governs the imprecision in the internal representation, and a second parameter
397 corresponds to additional response noise: the motor noise, parameterized by σ_0^2 , in the
398 estimation task, and the lapse probability, η , in the discrimination task. The behavior of the
399 model, across the two tasks and the different priors, reproduces that of the subjects (Figs. 1c
400 and 2c, dotted lines). In the estimation task, the standard deviation of estimates increases
401 as a function of the prior width, as it does in subjects’ responses. The Fisher information in
402 this model is constant with respect to x , and thus the variance of the internal representation,
403 r , is also constant; but the Bayesian estimate, $x^*(r)$, depends on the prior, and its variability
404 decreases for numerosities closer to the edges of the uniform prior. Hence the standard
405 deviation of the model’s estimates adopts an inverted U-shape similar to that of the subjects
406 (Fig. 1c). In the discrimination task, the model’s choice-probability curve is steeper in the
407 Narrow condition than in the Wide condition, and the two predicted curves are close to
408 the subjects’ choice probabilities (Fig. 2c). We emphasize that how the internal imprecision
409 scales with the prior width is entirely determined by our theoretical predictions (Eq. 8);
410 these quantitative predictions allow our model to capture the subjects’ imprecise responses
411 simultaneously across different priors.

412 Discussion

413 In this study, we examine the variability in subjects' responses in two different tasks and
414 with different priors. We find that the precision of their responses depends both on the task
415 and on the prior. The scale of their imprecision about the presented numbers increases sub-
416 linearly with the width of the prior, and this sublinear relation is different in each task. The
417 two sublinear relations are predicted by a resource-rational account, whereby the allocation
418 of encoding resources optimizes a tradeoff, maximizing each task's expected reward while
419 incurring a cost on the activity of the encoding neurons. Different formalizations of this
420 tradeoff suggested in several other studies cannot reproduce our experimental findings.

421 The model and the data suggest a scaling law relating the size of the representations'
422 imprecision to the width of the prior, with an exponent that depends on the task at hand.
423 An important implication is that the relative precision with which people represent external
424 information can be modulated by their objective and by the manner and the context in which
425 the representations are elicited. In the model, the scaling law results from the solution
426 to the encoding allocation problem (Eq. 6) in the special case of a uniform prior, and in
427 the contexts of estimation and discrimination tasks. We surmise that with non-uniform
428 priors and with other tasks (that imply different expected-reward functions), the behavior
429 of subjects should be consistent with the optimal solution to the corresponding resource-
430 allocation problem, provided that subjects are able to learn these other priors and objectives.
431 Further investigations of this conjecture will be crucial in order to understand the extent
432 to which the formalism of optimal resource-allocation that we present here might form a
433 fundamental component in a comprehensive theory of the brain's internal representations of
434 magnitudes.

435 References

- 436 [1] Tobias Bothwell, Colin J. Kennedy, Alexander Aeppli, Dhruv Kedar, John M. Robinson,
437 Eric Oelker, Alexander Staron, and Jun Ye. Resolving the gravitational redshift across
438 a millimetre-scale atomic sample. *Nature*, 602(7897):420–424, 2022.

- 439 [2] L. L. Thurstone. Psychophysical Analysis. *The American Journal of Psychology*,
440 38(3):368, jul 1927.
- 441 [3] Wilson P. Tanner and John A. Swets. A decision-making theory of visual detection.
442 *Psychological Review*, 61(6):401–409, 1954.
- 443 [4] George A. Gescheider. *Psychophysics*. Psychology Press, jun 1997.
- 444 [5] D. H. Hubel and T. N. Wiesel. Receptive fields of single neurones in the cat’s striate
445 cortex. *The Journal of Physiology*, 148(3):574–591, oct 1959.
- 446 [6] G. H. Henry, B. Dreher, and P. O. Bishop. Orientation specificity of cells in cat striate
447 cortex. *Journal of Neurophysiology*, 37(6):1394–1409, 1974.
- 448 [7] KH Britten, MN Shadlen, WT Newsome, and JA Movshon. The analysis of visual
449 motion: a comparison of neuronal and psychophysical performance. *The Journal of*
450 *Neuroscience*, 12(12):4745–4765, dec 1992.
- 451 [8] E. L. Kaufman, M. W. Lord, T. W. Reese, and J. Volkmann. The Discrimination of
452 Visual Number. *The American Journal of Psychology*, 62(4):498, oct 1949.
- 453 [9] Robert S. Moyer and Thomas K. Landauer. Time required for Judgements of Numerical
454 Inequality. *Nature*, 215(5109):1519–1520, sep 1967.
- 455 [10] Andreas Nieder and Earl K. Miller. Coding of cognitive magnitude: Compressed scaling
456 of numerical information in the primate prefrontal cortex. *Neuron*, 37(1):149–157, 2003.
- 457 [11] Esther F. Kutter, Jan Bostroem, Christian E. Elger, Florian Mormann, and Andreas
458 Nieder. Single Neurons in the Human Brain Encode Numbers. *Neuron*, 100(3):753–
459 761.e4, 2018.
- 460 [12] Stanislas Dehaene. *The Number Sense: How the Mind Creates Mathematics*. Oxford
461 University Press, New York, dec 2011.
- 462 [13] H. B. Barlow. Possible Principles Underlying the Transformations of Sensory Messages.
463 In Walter A. Rosenblith, editor, *Sensory Communication*, chapter 13, pages 217–234.
464 The MIT Press, Cambridge, MA, sep 1961.
- 465 [14] Nicolas Brunel and Jean-Pierre Nadal. Optimal tuning curves for neurons spiking as a
466 Poisson process. *Proceedings of the ESANN Conference*, 1997.
- 467 [15] Mark D. McDonnell and Nigel G. Stocks. Maximally Informative Stimuli and Tuning
468 Curves for Sigmoidal Rate-Coding Neurons and Populations. *Physical Review Letters*,
469 101(5):058103, aug 2008.
- 470 [16] Deep Ganguli and Eero P Simoncelli. Implicit encoding of prior probabilities in optimal
471 neural populations. In J. D. Lafferty, C. K. I. Williams, J. Shawe-Taylor, R. S. Zemel,
472 and A. Culotta, editors, *Advances in Neural Information Processing Systems 23*, pages
473 658—666. Curran Associates, Inc., 2010.

- 474 [17] Deep Ganguli and Eero P. Simoncelli. Efficient Sensory Encoding and Bayesian Inference
475 with Heterogeneous Neural Populations. *Neural Computation*, 26(10):2103–2134, oct
476 2014.
- 477 [18] Xue-Xin Wei and Alan A. Stocker. A Bayesian observer model constrained by efficient
478 coding can explain 'anti-Bayesian' percepts. *Nature Neuroscience*, 18(10):1509–1517,
479 oct 2015.
- 480 [19] Xue-Xin Wei and Alan A Stocker. Mutual Information, Fisher Information, and Efficient
481 Coding. *Neural Computation*, 326:305–326, 2016.
- 482 [20] Deep Ganguli and Eero P. Simoncelli. Neural and perceptual signatures of efficient
483 sensory coding. *ArXiv e-prints*, pages 1–24, feb 2016.
- 484 [21] Zhuo Wang, Alan A. Stocker, and Daniel D. Lee. Efficient Neural Codes That Minimize
485 Lp Reconstruction Error. *Neural Computation*, 28(12):2656–2686, dec 2016.
- 486 [22] Il Memming Park and Jonathan W. Pillow. Bayesian Efficient Coding. *bioRxiv*, 2017.
- 487 [23] Michael Morais and Jonathan W Pillow. Power-law efficient neural codes provide general
488 link between perceptual bias and discriminability. *Advances in Neural Information
489 Processing Systems 31*, 2(1):5076–5085, 2018.
- 490 [24] Arthur Prat-Carrabin and Michael Woodford. Bias and variance of the Bayesian-mean
491 decoder. In M Ranzato, A Beygelzimer, Y Dauphin, P S Liang, and J Wortman
492 Vaughan, editors, *Advances in Neural Information Processing Systems*, volume 34, pages
493 23793–23805. Curran Associates, Inc., 2021.
- 494 [25] Ling Qi Zhang and Alan A. Stocker. Prior Expectations in Visual Speed Perception
495 Predict Encoding Characteristics of Neurons in Area MT. *The Journal of neuroscience
496 : the official journal of the Society for Neuroscience*, 42(14):2951–2962, 2022.
- 497 [26] Ahna R Girshick, Michael S Landy, and Eero P Simoncelli. Cardinal rules: visual orien-
498 tation perception reflects knowledge of environmental statistics. *Nature Neuroscience*,
499 14(7):926–932, jul 2011.
- 500 [27] Samuel J. Cheyette and Steven T. Piantadosi. A unified account of numerosity percep-
501 tion. *Nature Human Behaviour*, 2020.
- 502 [28] Arthur Prat-Carrabin and Michael Woodford. Efficient coding of numbers explains
503 decision bias and noise. *Nature Human Behaviour*, pages 845–848, may 2022.
- 504 [29] Falk Lieder and Thomas L. Griffiths. Resource-rational analysis: Understanding human
505 cognition as the optimal use of limited computational resources. *Behavioral and Brain
506 Sciences*, 43:e1, feb 2020.
- 507 [30] Wei Ji Ma and Michael Woodford. Multiple conceptions of resource rationality. *Behav-
508 ioral and Brain Sciences*, 43:e15, mar 2020.

- 509 [31] Jonathan Schaffner, Sherry Dongqi Bao, Philippe N. Tobler, Todd A. Hare, and Rafael
510 Polania. Sensory perception relies on fitness-maximizing codes. *Nature Human Be-*
511 *haviour*, 7(7):1135–1151, 2023.
- 512 [32] S B Laughlin, R R de Ruyter Van Steveninck, and J C Anderson. The metabolic cost
513 of neural information. *Nature neuroscience*, 1(1):36–41, 1998.
- 514 [33] Andrea Hasenstaub, Stephani Otte, Edward Callaway, and Terrence J. Sejnowski.
515 Metabolic cost as a unifying principle governing neuronal biophysics. *Proceedings of the*
516 *National Academy of Sciences of the United States of America*, 107(27):12329–12334,
517 2010.
- 518 [34] Biswa Sengupta, Martin Stemmler, Simon B. Laughlin, and Jeremy E. Niven. Action
519 potential energy efficiency varies among neuron types in vertebrates and invertebrates.
520 *PLoS Computational Biology*, 6(7):35, 2010.
- 521 [35] Véronique Izard and Stanislas Dehaene. Calibrating the mental number line. *Cognition*,
522 106(3):1221–1247, 2008.
- 523 [36] Alberto Testolin and James L. McClelland. Do estimates of numerosity really adhere to
524 Weber’s law? A reexamination of two case studies. *Psychonomic Bulletin and Review*,
525 28(1):158–168, 2021.
- 526 [37] Camillo Padoa-Schioppa. Range-adapting representation of economic value in the or-
527 bitofrontal cortex. *Journal of Neuroscience*, 29(44):14004–14014, 2009.
- 528 [38] Shunsuke Kobayashi, Ofelia Pinto de Carvalho, and Wolfram Schultz. Adaptation of
529 Reward Sensitivity in Orbitofrontal Neurons. *The Journal of Neuroscience*, 30(2):534–
530 544, jan 2010.
- 531 [39] Xinying Cai and Camillo Padoa-Schioppa. Neuronal encoding of subjective value in
532 dorsal and ventral anterior cingulate cortex. *Journal of Neuroscience*, 32(11):3791–
533 3808, 2012.
- 534 [40] Alireza Soltani, Benedetto De Martino, and Colin Camerer. A Range-Normalization
535 Model of Context-Dependent Choice: A New Model and Evidence. *PLoS Computational*
536 *Biology*, 8(7):e1002607, jul 2012.
- 537 [41] Antonio Rangel and John A. Clithero. Value normalization in decision making: Theory
538 and evidence. *Current Opinion in Neurobiology*, 22(6):970–981, 2012.
- 539 [42] Kenway Louie and Paul W. Glimcher. Efficient coding and the neural representation of
540 value. *Annals of the New York Academy of Sciences*, 1251(1):13–32, mar 2012.
- 541 [43] Gideon Schwarz. Estimating the Dimension of a Model. *The Annals of Statistics*,
542 6(2):461–464, mar 1978.
- 543 [44] Robert E. Kass and Adrian E. Raftery. Bayes Factors. *Journal of the American Statis-*
544 *tical Association*, 90(430):773–795, jun 1995.

- 545 [45] Norberto M. Grzywacz and Rosario M. Balboa. A Bayesian framework for sensory
546 adaptation. *Neural Computation*, 14(3):543–559, 2002.
- 547 [46] Alan A. Stocker and Eero P. Simoncelli. Sensory adaptation within a Bayesian frame-
548 work for perception. *Advances in Neural Information Processing Systems*, 18:1291–1298,
549 2006.
- 550 [47] Alan A. Stocker and Eero P. Simoncelli. Noise characteristics and prior expectations in
551 human visual speed perception. *Nature Neuroscience*, 9(4):578–585, apr 2006.

552 **Methods**

553 **Estimation task**

554 **Task and subjects** 36 subjects (20 female, 15 male, 1 non-binary) participated in the
555 estimation-task experiment (average age: 21.4, standard deviation: 2.8). The experiment
556 took place at Columbia University, and complied with the relevant ethical regulations; it was
557 approved by the university’s Institutional Review Board (protocol number: IRB-AAAS8409).
558 All subjects experienced the three conditions.

559 In the experiment, subjects provide their responses using a slider (Fig. 1a), whose size
560 on screen is proportional to the width of the prior. Each condition comprises three different
561 phases. In all the trials of all three phases the numerosities are randomly sampled from
562 the prior corresponding to the current condition. This prior is explicitly told to the subject
563 when the condition starts. In each of the 15 trials of the first, ‘learning’ phase, the subject
564 is shown a cloud of dots together with the number of dots it contains (i.e., its numerosity
565 represented with Arabic numerals). These elements stay on screen until the subject chooses
566 to move on to the next trial. No response is required from the subject in this phase. Then
567 follow the 30 trials of the ‘feedback’ phase, in which clouds of dots are shown for 500ms
568 without any other information on their numerosities. The subject is then asked to provide
569 an estimate of the numerosity. Once the estimate is submitted, the correct number is shown
570 on screen. The third and last phase is the ‘no-feedback’ phase, which is identical to the

571 ‘feedback’ phase, except that no feedback is provided. In both the ‘feedback’ phase and the
572 ‘no-feedback’ phase, subjects respond at their own pace. All the analyses presented here use
573 the data of the ‘no-feedback’ phase, which comprises 120 trials.

574 At the end of the experiment, subjects receive a financial reward equal to the sum of a
575 \$5 show-up fee (USD) and of a performance bonus. After each submission of an estimate,
576 an amount equal to $0.10 - (\hat{x} - x)^2/600$, where x is the correct number and \hat{x} the estimate,
577 is added to the performance bonus. If at the end of the experiment the performance bonus
578 is negative, it is set to zero. The average reward was \$11.80 (standard deviation: 6.98).

579 **Bins defined over the priors, and calculation of the variance** The ranges of the
580 three priors (50-70, 40-80 and 30-90), contain 21, 41, and 61 integers, respectively, and thus
581 none of them can be split in five bins containing the same number of integers. Hence the
582 ranges defining each of the five bins were chosen such that the third bin contains an odd
583 number of integers, with at its middle the middle number of the prior (60 in each case), and
584 such that the second and fourth bins contain the same number of integers as the third one;
585 the first and last bins then contain the remaining integers. In the Narrow condition, the
586 ranges of the five bins are: 50-52, 53-57, 58-62, 63-67, and 68-70. In the Medium condition,
587 the ranges of the five bins are: 40-46, 47-55, 56-64, 65-73, and 74-80. In the Wide condition,
588 the ranges of the five bins are: 30-40, 41-53, 54-66, 67-79, and 80-90.

589 In our calculation of the variance of estimates, when pooling responses by bins of pre-
590 sented numbers, we do not wish to include the variability stemming from the diversity of
591 numbers in each bin. Thus we subtract from each estimate \hat{x} of a number the average of all
592 the estimates obtained with the same number, $\langle \hat{x} \rangle$. The calculation of the variance for a bin
593 then makes use of these ‘excursions’ from the mean estimates, $\hat{x} - \langle \hat{x} \rangle$.

594 **Model fitting and individual subjects analysis** The Gaussian-representation model
595 used throughout the text has three parameters: α , ν , and σ_0 . We fit these parameters to
596 the subjects’ data by maximizing the model’s likelihood. For each parameter, we can either

α	ν	σ_0	Num. param.	BIC
Fixed $\alpha = 1$	Shared	Shared	2	81762.79
Fixed $\alpha = 1/2$	Shared	Shared	2	*81519.07
Shared ($\alpha = .48$)	Shared	Shared	3	81527.78
Fixed $\alpha = 1$	Indiv.	Shared	37	81729.64
Fixed $\alpha = 1$	Shared	Indiv.	37	81746.34
Fixed $\alpha = 1$	Indiv.	Indiv.	72	81657.67
Fixed $\alpha = 1/2$	Indiv.	Shared	37	81427.11
Fixed $\alpha = 1/2$	Shared	Indiv.	37	81467.71
Fixed $\alpha = 1/2$	Indiv.	Indiv.	72	*81346.37
Shared ($\alpha = .43$)	Indiv.	Shared	38	81437.93
Shared ($\alpha = .45$)	Shared	Indiv.	38	81472.85
Shared ($\alpha = .44$)	Indiv.	Indiv.	73	81350.90
Indiv.	Shared	Shared	38	81444.60
Indiv.	Indiv.	Shared	73	81571.48
Indiv.	Shared	Indiv.	73	81366.40
Indiv.	Indiv.	Indiv.	108	81453.52

Table 1. Estimation task: model fitting supports the hypothesis $\alpha = 1/2$, both with pooled and individual responses. Number of parameters (second-to-last column) and BIC (last column) of the Gaussian-representation model under different specifications regarding whether all subjects share the same values of the three parameters α , ν , and σ_0 (first three columns). ‘Shared’ indicates that the responses of all the subjects are modeled with the same value of the parameter. ‘Indiv.’ indicates that different values of the parameter are allowed for different subjects. For the parameter α , ‘Fixed’ indicates that the value of α is fixed (thus it is not a free parameter); when the parameter α is ‘Shared’, it is a free parameter, and we indicate its best-fitting value in parentheses. In the first three lines of the table, all three parameters are shared across the subjects (the three lines differ only by the specification of α); while in the remaining lines at least one parameter is individually fit. In both cases the lowest BIC (indicated by a star) is obtained for a model with a fixed parameter $\alpha = 1/2$.

597 allow for ‘individual’ values of the parameter that may be different for different subjects, or
598 we can fit the responses of all the subjects with the same, ‘shared’ value of the parameter.
599 In the main text we discuss the model with ‘shared’ parameters; the corresponding BICs
600 are shown in the first three lines of Table 1. The other lines of the Table correspond to
601 specifications of the model in which at least one parameter is allowed to take ‘individual’
602 values. In both cases the lowest BIC is obtained for models with a fixed exponent $\alpha = 1/2$,
603 common to all the subjects, consistently with our prediction (Eq. 8). Overall, the best-fitting

604 model allows for ‘individual’ values of the parameters ν and σ_0 , and a fixed, shared value
605 for α . This suggests that the parameters ν and σ_0 , which govern, respectively, the degrees
606 of “internal” and “external” (motor) imprecision, capture individual traits characteristic of
607 each subject, while the exponent α reflects the solution to the optimization problem posed
608 by the task, which is the same for all the subjects.

609 **Discrimination task**

610 **Task and subjects** 111 subjects (61 male, 50 female) participated in the discrimination-
611 task experiment (average age: 31.4, standard deviation: 10.2). Due to the COVID crisis, the
612 experiment was run online, and each subject experienced only one condition. 31 subjects
613 participated in the Narrow condition, and 32 subjects participated in the Wide condition.
614 This experiment was approved by Columbia University’s Internal Review Board (protocol
615 number: IRB-AAAR9375).

616 In this experiment, each condition starts with 20 practice trials. In each of these trials,
617 five red numbers and five blue numbers are shown to the subject, each for 500ms. In the
618 first 10 practice trials, no response is asked from the subject. In the following 10 practice
619 trials, the subject is asked to choose a color; choices in these trials do not impact the reward.
620 Then follow 200 ‘real’ trials in which the averages chosen by the subject are added to a score.
621 At the end of the experiment, the subject receives a financial reward that is the sum of a
622 \$1.50 fixed fee (USD) and of a non-negative variable bonus. The variable bonus is equal to
623 $\max(0, 1.6(\text{AverageScore} - 50))$, where AverageScore is the score divided by 200. The average
624 reward was \$6.80 (standard deviation: 2.15).

625 **Individual subjects analysis** In the Gaussian-representation model, a numerosity x
626 yields a representation that is normally-distributed, as $r|x \sim N(x, \nu^2 w^{2\alpha})$. Fitting the model
627 to the pooled data collected in the two conditions has enabled us to identify separately the
628 two parameters ν and α . But fitting to the responses of individual subjects, who experienced

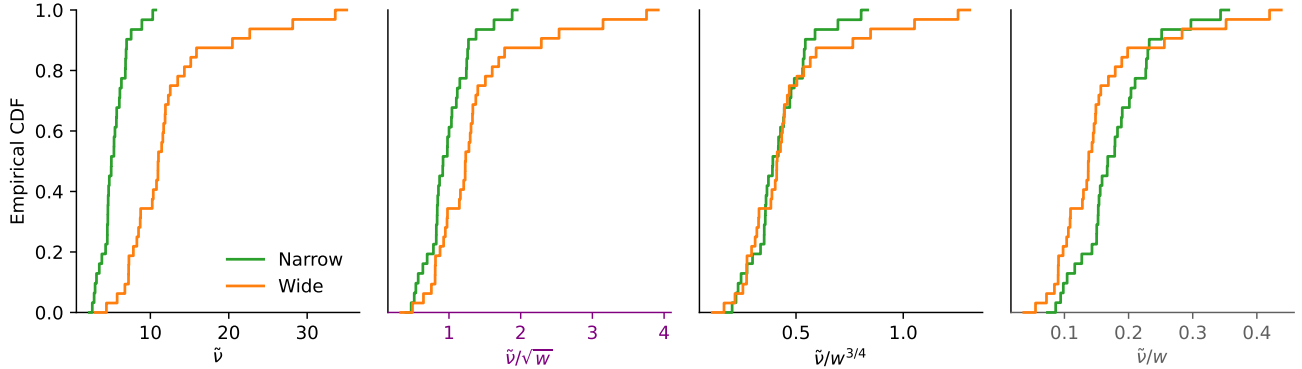


Fig. 3. Discrimination task: empirical across-subjects distribution of scaled best-fitting standard-deviation parameter. The first panel shows the empirical cumulative distribution function (CDF) of the fitted parameter $\tilde{\nu}$, unscaled. The second, third, and fourth panels show the empirical CDF of $\tilde{\nu}$ divided by w^α , with $\alpha = 1/2$, $3/4$, and 1 , respectively.

629 only one of the two conditions, only allows to identify the variance $\tilde{\nu}^2 \equiv \nu^2 w^{2\alpha}$, and not ν
630 and α separately. However, an important difference between these two parameters is that
631 the baseline variance ν^2 is idiosyncratic to each subject (and thus we expect inter-subject
632 variability for this parameter), while the exponent α , in our theory, is determined by the
633 specifics of the task, and thus it should be the same for all the subjects; in particular, we
634 predict $\alpha = 3/4$. Therefore, as subjects were randomly assigned to one of the two conditions,
635 we expect the distribution of $\nu = \tilde{\nu}/w^\alpha$ to be identical across the two conditions. We thus
636 look at the empirical distributions of this quantity, with different values of α , in the two
637 conditions. We find that the distributions of $\tilde{\nu}$, $\tilde{\nu}/\sqrt{w}$, and $\tilde{\nu}/w$, in the two conditions, do
638 not match well; but the distributions of $\tilde{\nu}/w^{3/4}$ in the two conditions are close to each other
639 (Fig. 3). In each of these four cases, we run a Kolmogorov-Smirnov test of the equality of the
640 underlying distributions. With $\tilde{\nu}$, $\tilde{\nu}/\sqrt{w}$, and $\tilde{\nu}/w$, the null hypothesis is rejected (p-values:
641 $1e-10$, 0.008 , and 0.001 , respectively), while with $\tilde{\nu}/w^{3/4}$ the hypothesis (of equality of the
642 distributions in the two conditions) is not rejected (p-value: 0.79). Thus this analysis, based
643 on the individual model-fitting of the subjects, substantiates our conclusions.

644 **Models' BICs** We fit the Gaussian-representation model, with or without lapses, to the
645 subjects' responses in the discrimination task. In the main text we discuss the model-fitting
646 results of the model with lapses. The corresponding BICs are reported in the last four lines of
647 Table 2, while the first four lines report the BICs of the model with no lapses. Table 2 shows
648 that including lapses in the model yields lower BICs, but also that in both cases (with or
649 without lapses), the lowest BIC is obtained with the model with a fixed parameter $\alpha = 3/4$,
650 consistently with our theoretical prediction (Eq. 8).

α	Lapses	Num. param.	BIC
Fixed $\alpha = 1$	No	1	11737.03
Fixed $\alpha = 3/4$	No	1	*11721.22
Fixed $\alpha = 1/2$	No	1	11815.86
Free ($\alpha = .84$)	No	2	11723.22
Fixed $\alpha = 1$	Yes	2	11635.59
Fixed $\alpha = 3/4$	Yes	2	*11617.24
Fixed $\alpha = 1/2$	Yes	2	11661.35
Free ($\alpha = .80$)	Yes	3	11625.14

Table 2. Discrimination task: model fitting supports the hypothesis $\alpha = 3/4$. Number of parameters (second-to-last column) and BIC (last column) of the Gaussian-representation model under different specifications regarding the parameter α (first column) and the absence or presence of lapses (second column). In the bottom four lines the model features lapses, while it does not in the top four lines; in both cases the lowest BIC (indicated with a star) is obtained with the specification $\alpha = 3/4$.

651 **Data availability statement**

652 Requests for the data can be sent via email to the corresponding author.

653 **Code availability statement**

654 Requests for the code used for all analyses can be sent via email to the corresponding author.

655 **Acknowledgments**

656 We thank Jessica Li and Maggie Lynn for their help as research assistants, Hassan Afrouzi
657 for helpful comments, and the National Science Foundation for research support (grant SES
658 DRMS 1949418).

659 **Competing interest declaration**

660 The authors declare no conflict of interest.